International Journal of Pharmaceutics 403 (2011) 245–253

Contents lists available at ScienceDirect

International Journal of Pharmaceutics

journal homepage: www.elsevier.com/locate/ijpharm

Pharmaceutical Nanotechnology

Entrapment and release difference resulting from hydrogen bonding interactions in niosome

Yong-Mei Hao[a,*], Ke'an Li[b]

[a] College of Chemistry and Chemical Engineering, Graduate University of Chinese Academy of Sciences, 19(A) Yu Quan Road, Beijing 100049, China
[b] College of Chemistry and Molecular Engineering, Peking University, Beijing 100871, China

ARTICLE INFO

Article history:
Received 20 July 2010
Received in revised form 8 October 2010
Accepted 18 October 2010
Available online 31 October 2010

Keywords:
Niosome
Drug carrier
Hydrogen bonding interaction
Salicylic acid
p-Hydroxyl benzoic acid

ABSTRACT

In this study the influence of hydrogen bonding interaction between niosomal membrane and solutes on the drug loading and release was investigated. Salicylic acid (SA) and *p*-hydroxyl benzoic acid (*p*-BA) were selected as models. Niosomes were prepared with 1:1 molar ratios of various surfactants and cholesterol by film hydration technique, and the corresponding formulation variables were optimized to achieve the maximum entrapment efficiencies (EE%). The EE% of different formulations followed the trend Span 60 > Span 40 > Span 20 > Span 80. Additionally, it was also found that the EE% of *p*-BA was much higher than that of SA. This difference may be due to the formation of hydrogen bond between *p*-BA and niosomal membrane, and the corresponding interaction diagram has been proposed and confirmed indirectly by UV spectroscopy method. The quantitative analysis of hydrogen binding interaction between solutes and niosome has been finished firstly, and the corresponding entrapment equilibrium constant K has been calculated as well. Moreover, in vitro the release of both drugs from niosomes was examined in simulated gastric fluid (SGF) and simulated intestinal fluid (SIF), respectively. The results indicated that the release of *p*-BA in SIF was much slower than that in SGF, and the release rate of SA in SGF is apparently slower than that in SIF. The possible mechanism was given as well.

1. Introduction

Direct delivery of some active drugs through the cell membrane into cells was generally inefficient and often faced with many problems, such as enzymolysis, hydrolysis, severely toxic-side effects and so on. Niosome, one kind of colloidal particles, can encapsulate these active drugs, and brings a very promising way to increase drug bioavailability, prevent drug degradation, reduce drug toxic effects and transport drugs to the target sites (Azmin et al., 1985; Bandak et al., 1999). Moreover, niosome attracts much attention because of its advantages in many aspects, such as chemical stability, high purity, content uniformity, low cost and convenient storage of non-ionic surfactants, and large numbers of surfactants available for the design of niosomes (Vora et al., 1998). In the past two decades, niosomes have been proposed for many potential therapeutic applications, i.e. as the tumor targeting agent (Hong et al., 2009), diagnostic imaging agents (Uchegbu and Vyas, 1998), drug carriers of anticancer drug (Bayindir and Yuksel, 2010; Gude et al., 2002), antifungal drug (Barakat et al., 2009), anti-inflammatory drug (Alsarra, 2009) and so on.

As a drug carrier, encapsulating a sufficient amount of the therapeutic agent is one of the most desirable properties for niosomes usage (Mainardes and Silva, 2004; Manconi et al., 2006). Up to now, various techniques have been used to optimize drug loading and release. Totally, factors affecting the encapsulation efficiency of niosomes consist of three main areas, namely, the nature of the niosomes, the nature of drugs, interaction between niosomes and drugs (Shi et al., 2006). Take into account the nature of the niosomes, some factors affect the encapsulation efficiency (EE), including niosome preparation method (Aggarwal et al., 2004; Arunothayanun et al., 1999), cholesterol content (Assadullahi et al., 1991; Nasr et al., 2008), the nature of surfactants (Bandyopadhyay and Johnson, 2007; Manosroi et al., 2005). As for the encapsulated drugs, the interaction between drug molecules, drug hydrophilic or lipophilic properties will influence the drug encapsulation efficiency, and the soluble drugs usually have a relatively low EE value in a number of formulations (Manosroi et al., 2008). Regarding the third aspect, several reported niosome systems have revealed that niosome membranes can interact with drug molecules *via* electrostatic interaction or other types of interaction, such as Van der Waals forces and hydration bridges (Paolino et al., 2007), these interactions have a significant impact on the encapsulation efficiency (Abd-Elbary et al., 2008; Junyaprasert et al., 2008; Paolino et al., 2008; Pardakhty et al., 2007). However, the majority of proposed niosome systems were only focused on the properties of

* Corresponding author. Tel.: +86 10 88256414; fax: +86 10 88256093.
E-mail address: ymhao@gucas.ac.cn (Y.M. Hao).

0378-5173/$ – see front matter © 2010 Elsevier B.V. All rights reserved.
doi:10.1016/j.ijpharm.2010.10.027

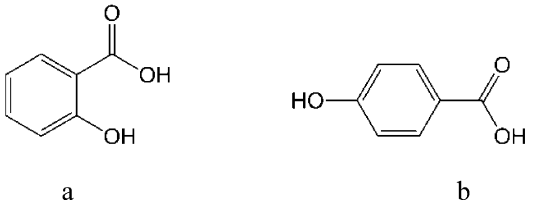

Chart 1. The structures of salicylic acid (a) and *p*-hydroxyl benzoic acid (b).

niosome and nature of drugs, the particular influence of interaction between membrane and solutes on drug encapsulation capacity and release properties have not been elucidated completely yet.

To rationally select or synthesize the appropriate surfactant and build highly efficient niosomal systems, it is necessary to consider the relationship between niosome membrane and drugs (Shi et al., 2006). Our previous research indicated that there was interaction between membrane and incorporated colchicine (Hao et al., 2002). To further explore some factors that affect the drug loading and release processes of niosome system, here salicylic acid (SA) and its isomer *p*-hydroxyl benzoic acid (*p*-BA) have been used as model solutes (Chart 1), sorbitan monolaurate (Span 20), monopalmitate (Span 40), monostearate (Span 60) and monooleate (Span 80) were used as surfactants (Chart 2). SA and *p*-BA have the same molecular weight but their hydroxyl and carboxyl groups located at different positions on the benzene ring, which may result in distinguishable interactions between niosome membrane and both solutes. The aim of this work is to investigate how the interaction between solute and membrane affects the entrapment capacity and solute release process. Some other factors, including surfactant structure, lipid concentration, solute content and dicetyl phosphate (DCP), have been examined and optimized as well. One probable mechanism to explain the difference in encapsulation and release between the two solutes has been suggested.

2. Materials and methods

2.1. Materials

SA and *p*-BA were products of Serva. Dicetyl phosphate (DCP), Span 20, Span 40, Span 60, and Span 80 were purchased from Sigma–Aldrich (USA) and used as received, while cholesterol (CH) was obtained from Beijing Chemical Reagent Company (China). Dialysis membrane tube (MW cut off 8000–10,000) was obtained from Sino-American Biotechnology Company (China) and was treated prior to use according to the reported method (Fenton et al., 1997). All other reagents were of analytical grade. Double-distilled water was used throughout the study.

2.2. Preparation of niosomes

Niosomes were prepared by film hydration method. Appropriate amount of Span dissolved in 10.0 mL of ethanol/chloroform

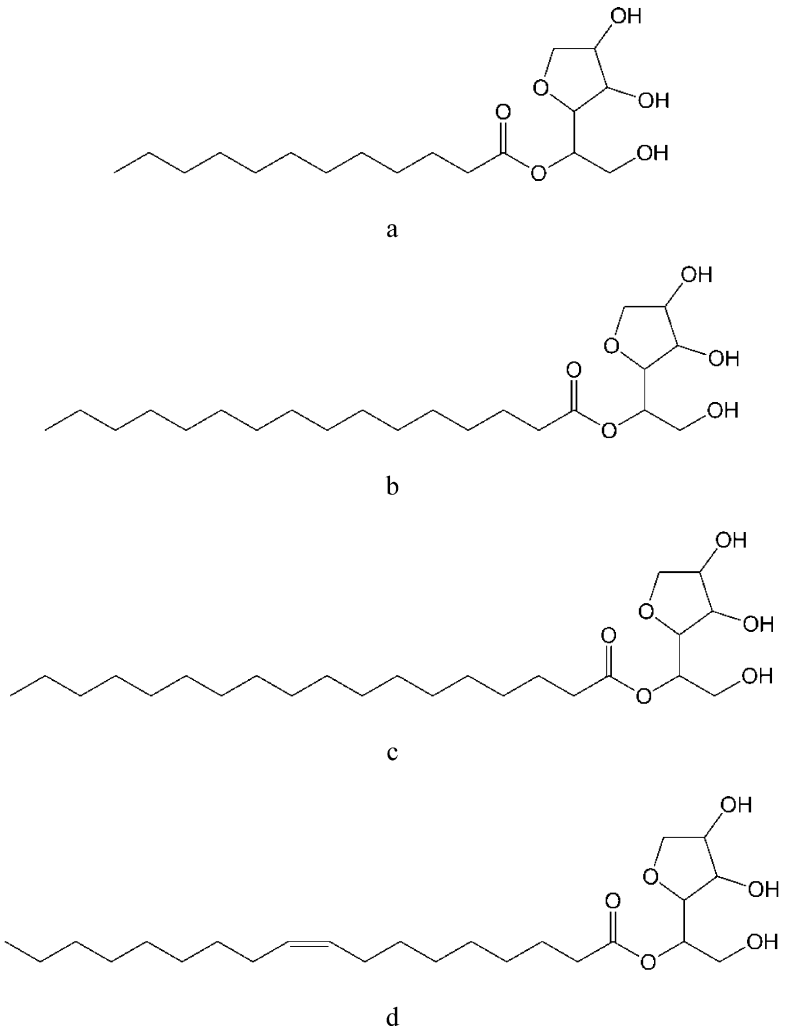

Chart 2. The structures of Span 20 (a), Span 40 (b), Span 60 (c), and Span 80 (d).

mixture (1:4, v/v), placed in a 100 mL round bottom flask. Afterwards, CH dissolved in chloroform was added. The organic solvent was removed under vacuum by a rotary evaporator (RE-52A, Shanghai Yarong Biochemistry Apparatus Ltd., China) at 60 °C to form a thin film on the wall of the flask. Residual chloroform was evaporated 4–8 h in vacuum at room temperature. The dried film was hydrated with 10 mL of SA solution at various concentrations ranged from 0 to 4.5×10^{-4} mol/L by 1 h sonication at 60 °C (Bath sonicator, Kunshan, Jiangsu, China). After preparation, the dispersion was left to equilibrate at room temperature overnight to ensure complete annealing and drugs distribution between the lipid bilayer and the aqueous phase. Niosomes containing *p*-BA were prepared in the same way. If the dried film was hydrated with 10 mL of water, the corresponding blank niosomes were prepared.

2.3. Characterization of prepared niosomes

Morphology analysis of niosomes was carried out by transmission electron microscopy (TEM) using a JEOL JEM-100S transmission electron microscope fitted with a LaB6 filament, with an operating voltage from 40 to 120 kV. A drop of the niosome colloidal suspension (10 μL) was placed on a carbon-coated copper grid and allowed to stand for 2 min. The excess of the niosome suspension was then removed by a piece of filter paper (Whatman Inc., Clifton, NJ, USA). A drop of negative stain solution, 2% (w/v) acetic uranium solution, was placed on the carbon grid thus staining the niosomes. After 1 min, the excess staining agent was removed by adsorbing the drop with the filter paper and the sample was then air-dried. The thin film of stained vesicles was viewed at an operating voltage of 70 kV with a transmission electron microscope.

The particle size in aqueous suspensions was also measured by dynamic light scattering (DLS) apparatus (NICOMP 380 ZLS, Particle Sizing Systems, Agilent Technologies, USA).

2.4. Stability of niosome systems

After solute loading, 100 mL of niosome solution was kept in glass bottles with plastic plugs and stored at 4° in the dark for 40 days to examine the stability of niosomes. The stability was evaluated by the mean values of EE % after 40 days.

2.5. Entrapment efficiency

Niosome-entrapped SA (SA-niosome) could be separated from untrapped SA by dialysis method (Mokhtar et al., 2008). The prepared niosomes were placed into dialysis bags and dialyzed for 24 h against 100 mL of phosphate buffer (PBS, pH 7.4). The amount of SA in dialysate (untrapped) was measured at 295 nm against PBS buffer (pH 7.4) as a blank (Shimadzu UV-265 spectrophotometer, Japan). The amount of entrapped SA could be obtained by subtracting amount of untrapped drug from the total drug used. The entrapment efficiency was defined as follows:

$$\text{entrapment efficiency\%} = \text{EE\%} = \frac{\text{amount of SA entrapped}}{\text{total amount of SA used}} \times 100\% \quad (1)$$

Similarly, *p*-BA-niosome could be obtained. The encapsulation efficiency of *p*-BA in niosome was determined based on the same method, and the amount of *p*-BA was determined spectrophotometrically at 247 nm.

2.6. Drug release study

In vitro release of SA/*p*-BA from niosomes was studied according to Hu's method with minor modification (Hu and Rhodes, 1999). Dialysis bag containing appropriate volume of SA/*p*-BA loaded niosome dispersion was placed in a flask containing 100 mL simulated gastric fluid (or simulated intestinal fluid): 0.05 M aqueous sodium chloride solution adjusted to pH 1.2 (821 acidometer, Zhongshan Univ., Guangzhou, China) with 1.0 M HCl as simulated gastric fluid (SGF) and 0.05 M potassium sodium dihydrogen phosphate buffer solution adjusted to pH 7.5 with 1.0 M NaOH as simulated intestinal fluid (SIF). The flask was placed on a shaker, and shaked at 37 °C at 50 rpm. Aliquots of dialysate were taken at predetermined time and replenished immediately with the same volume of fresh simulated fluid. The withdrawn samples were assayed spectrophotometrically at 295/247 nm to determine the release of SA/*p*-BA content. The fraction of SA release at specific time points was determined by comparing the released SA content with the total content of SA entrapped in niosomes. Release of free drug was studied in the same way.

According to the solubility of both drugs (0.2 g/100 g) (Speight, 2005), it only needs 0.1655 g water to dissolve 2.4×10^{-4} mol/L of both drugs. In this study, sink condition was achieved fully for both drugs before dialysis and maintained throughout the experiment since 100 mL of simulated fluid was used.

2.7. Investigation of absorption spectra

All niosome samples were prepared according to the method described in Section 2.2. Here in all niosome systems (Span 60:CH = 1:1), the concentration of total lipid was 2.0×10^{-4} mol/L. Based on their encapsulation efficiency, 10.0 mL of 1.3×10^{-4} mol/L SA solution was added initially when prepared SA-niosome while only the same volume of 9×10^{-5} mol/L *p*-BA solution was needed in preparing *p*-BA-niosome. SA-niosome/*p*-BA-niosome could be separated from untrapped SA/*p*-BA by dialysis method. Thus the concentration of SA and *p*-BA entrapped in niosome was 9×10^{-5} mol/L. The UV absorption spectra of free SA solution (9.0×10^{-5} mol/L), free *p*-BA solution (9.0×10^{-5} mol/L), SA-niosome, *p*-BA-niosome and blank niosome were recorded by a Shimadzu UV-265 spectrophotometer from 230 to 330 nm with a 1-cm path length cell, respectively.

2.8. Statistical analysis

The data were reported as mean ± S.D. ($n = 3$) and statistical analysis of the data was carried out using one way ANOVA followed by LSD test at a level of significant of $P < 0.05$.

3. Results and discussion

3.1. The morphology of prepared niosomes

TEM was used to investigate the morphology of prepared niosomes. It can be seen from Fig. 1a that all the niosomes were spherical and have a similar diameter of 130 nm, which is almost consistent with the result from laser particle analysis that gives an average hydrodynamic size of 151.1 ± 21.6 nm (Fig. 1b).

3.2. The influence of surfactant on drug loading

A series of niosomes of Span and CH (1:1) was prepared at the same total lipid concentration to investigate the influence of surfactant structure on niosomal properties. The encapsulation efficiency of four kinds of formulations was listed in Table 1, which indicated that Span 60 has significant higher entrapment efficiency than other Span types ($P < 0.05$). This could attribute to the surfactant chemical structure. Span 60 and Span 80 have the same head groups and same length of alkyl chain but Span 80 has an unsaturated double bonds. A previous report (Degier et al., 1968)

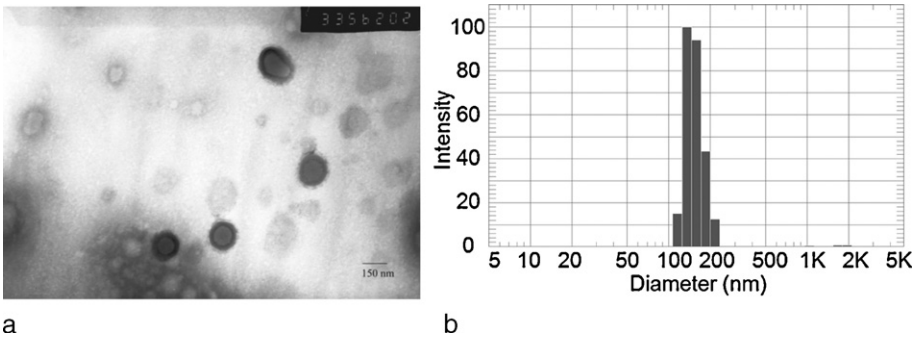

Fig. 1. TEM image (a) and particle size distribution (b) of niosomes. Concentrations of Span 60, cholesterol and SA remain at 1.00×10^{-4} mol/L, 1.00×10^{-4} mol/L and 9.0×10^{-5} mol/L, respectively.

Table 1
Percentage encapsulation efficiency (EE ± SD) of solutes in the niosomes.[a]

Span	Span 20	Span 40	Span 60	Span 80
EE of SA	27.0 ± 2.1	53.2 ± 2.9	68.8 ± 1.8	30.8 ± 3.0
EE of *p*-BA	90.0 ± 1.3	97.0 ± 2.0	100.0 ± 1.5	95.0 ± 1.9

[a] Concentration of total lipid and solute were 2.00×10^{-4} mol/L and 9.00×10^{-5} mol/L, respectively.

demonstrated that the introduction of double bonds into the paraffin chains causes a marked enhancement of the permeability of liposomes, possibly explaining the lowest entrapment of Span 80 formulation in this work. Considering the other three kinds of niosome formulations, all Span types have the same head group and alkyl chain in different length (Chart 2). Increase of the alkyl chain length leads to a higher entrapment efficiency, and the corresponding order follows the trend Span 60 (C16) > Span 40 (C14) > Span 20 (C12), which is consistent with other previous report (Mokhtar et al., 2008), suggesting that the length of alkyl chain is a crucial factor that should be considered in designing novel niosome system with high efficiency.

In addition, the four kinds of niosome formulations showed a different encapsulation capacity in loading SA and *p*-BA (Table 1), and lower SA contents were entrapped at the same experimental conditions ($P < 0.05$). As an isomer of SA, *p*-BA has the same molecular weight and functional groups but differ in the location of the functional group (Chart 1). The higher encapsulation capacity for *p*-BA indicates that the *p*-BA molecules greater affinity with the vesicle material, and the corresponding mechanism would be discussed later. To further investigate other factors on the encapsulation efficiency, formulation of Span 60/Span 80 and CH in a 1:1 molar ratio was used in the following experiments.

3.3. Impact of total lipid concentration

At first, we measured encapsulation efficiency of EE(*p*-BA) and EE(SA) with increasing total lipid concentration while keeping other factors unchanged. The values of EE(*p*-BA) almost kept constant (100%) in the range of 4.0×10^{-5} to 3.2×10^{-4} mol/L of total lipid, while it decreased 10% when the concentration of lipid reached 4.0×10^{-4} mol/L (Fig. 2a). The EE(SA) was increased from 51.2% to 68.8% as the lipid concentration was increased from 5.0×10^{-5} to 2.0×10^{-4} mol/L, respectively. On the other hand, the amount of SA entrapped was reduced to 52.5% when the total lipid concentration increased to 4.0×10^{-4} mol/L. The entrapment efficiency dropped 10% in Fig. 2a leads to the fact that the number of niosomes taking part in encapsulation decreases as increasing the lipid concentration, which might be ascribed to the aggregate of niosomes at high lipid level. In fact, white precipitate can be observed when the total lipid concentration reaches 1.0×10^{-3} mol/L. To confirm this point, influences of total concentration of Span 80 and CH on the inclusion of SA and *p*-BA were further investigated. As expected, the incorporation of SA and *p*-BA decreased both in dilute and thick lipid concentration (Fig. 2b) ($P < 0.05$). In this study, 2.0×10^{-4} mol/L of total lipid was chosen in later experiments. Under the same experimental condition, the entrapment efficiency of Span 60 formulations was higher than those of Span 80, which was similar to that in Section 3.2.

3.4. Effect of solute content

In this study, SA and *p*-BA were selected as model solutes. Some important applications of SA have been found in the aspects of treating skin disorders, such as acne, psoriasis, seborrheic dermatitis of the skin and scalp, calluses, corns, common warts, and plantar

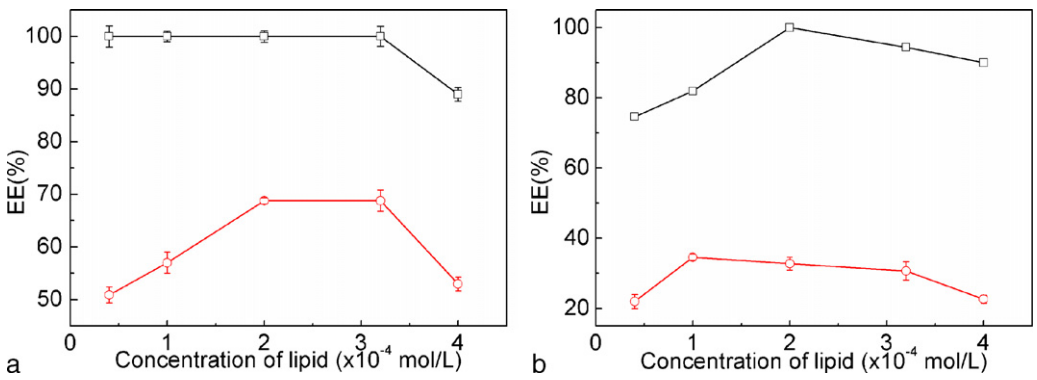

Fig. 2. Influence of total lipid concentration (Span and cholesterol) on entrapment efficiency of Span 60 (a) and Span 80 (b) formulation. Open square (□) and open circle (○) denote *p*-BA and SA, respectively. Concentration of both solutes was 9.00×10^{-5} mol/L.

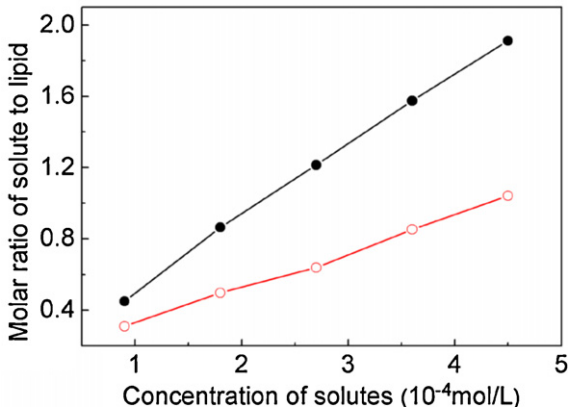

Fig. 3. Molar ratio ($R = M_{solute}/M_{lipid}$) of solute entrapped in niosomes (made up of Span 60 and CH) to total lipid. Solid circle (●) and open circle (○) denote *p*-BA and SA, respectively.

warts, depending on the dosage form and strength of the preparation. However, SA should be very cautiously employed because of its cardiac trouble risk and contraindication in diseased conditions of the kidneys. As to the isomeric compound of SA, *p*-BA has potential in the treatment of melanoma (Zhao et al., 1998).

To investigate the influence of drug dosage, the encapsulation capability of Span 60 formulation has been examined by varying the concentration of SA and *p*-BA while keeping the total level of lipid at 2×10^{-4} mol/L. With the increasing of solutes concentration, the ratio (R) of the loaded SA to total lipid increased linearly and reached about 1:1 when the concentration of SA was 4.5×10^{-4} mol/L (Fig. 3). Similarly, the ratio (R) of incorporated *p*-BA to lipid reached 2:1 at the same solute level (Fig. 3). Statistical analysis displayed that the differences in EE of the two solutes with the increasing solutes concentration from 1 to 4.5×10^{-4} mol/L were significant ($P < 0.05$). Moreover, in Span 80 case, the ratio (R) of the loaded SA to total lipid also increased linearly and reached about 0.5:1 while the ratio of entrapped *p*-BA to lipid reached 1.6:1. The amount of encapsulated drugs increased with increasing amount of drugs added during the preparation could be due to the saturation of the media with drugs that forces more drug's molecule to be entrapped into niosomes (EL-Samaligy et al., 2006; Mokhtar et al., 2008). The high ratio of entrapped solutes to lipid indicated that the niosomal formulation prepared in this study have a higher capability in encapsulation soluble drugs than some reported ones (Abd-Elbary et al., 2008; Arunothayanun et al., 2000; Paolino et al., 2008).

3.5. Influence of DCP

The effects of charge inducing agents on the EE% of model drugs in Span 60 and Span 80 formulations were checked. DCP, imparting negative charges on niosomes, usually used to prevent niosome aggregation and increase the stability of the niosomal dispersion. In this study, the incorporation of DCP resulted in a decrease in both EE% in examined formulations ($P < 0.05$). Both SA ($pK_{a1} = 2.97$, $pK_{a2} = 13.40$) and *p*-BA ($pK_{a1} = 4.48$, $pK_{a2} = 9.32$) are weak acids. Under the experimental condition (pH 7.4), the carboxyl group of both SA and *p*-BA would lose one proton and transform themselves into carboxylate anion. Obviously, the lower drug entrapment in the presence of DCP was due to the electrostatic repulsion forces between the carboxylate anion of both drugs and the anionic headgroup of DCP.

In addition, here DCP had no effect on the system stability. The value of EE% remained almost unchanged during a 40-day storage period in the absence and presence of DCP. Negatively charged SA or *p*-BA molecules encapsulated in niosome maybe stabilize the

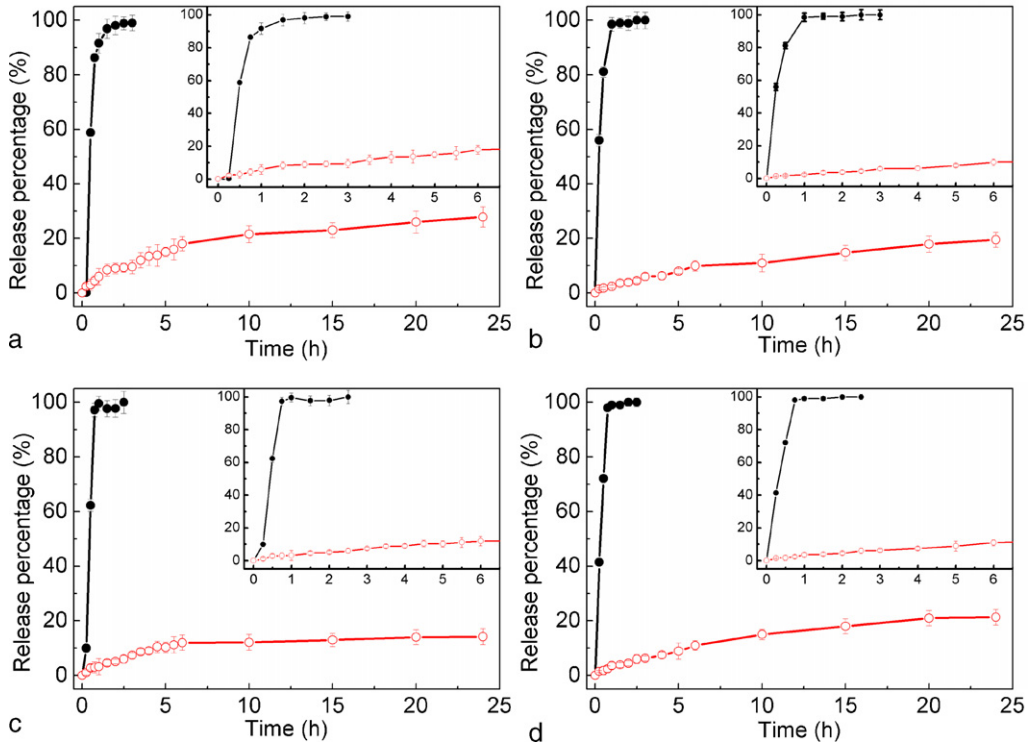

Fig. 4. Release percentage of SA (a) and *p*-BA (c) in SIF from free solution (solid circle) or from niosomal formulation (open circle), and release percentage of SA (b) and *p*-BA (d) in SGF from free solution (solid circle) or from niosomal formulation (open circle). Niosome was made up of 1.00×10^{-4} mol/L Span 60 and 1.00×10^{-4} mol/L cholesterol. The concentration of both solutes was 2.4×10^{-4} mol/L.

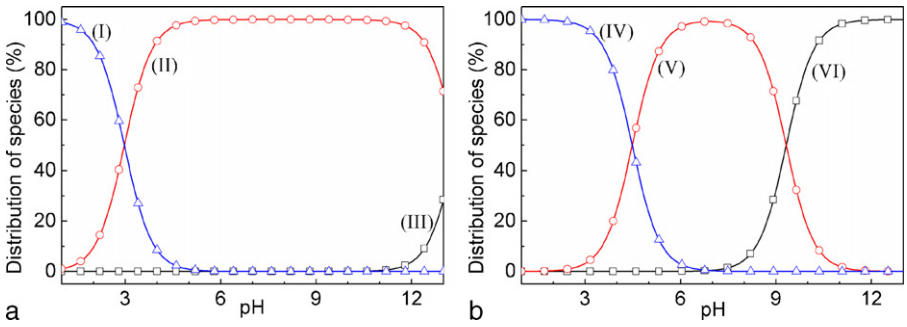

Fig. 5. Species distribution curves at different pH values. (a) SA and (b) *p*-BA. The structures of species (I) to (VI) were shown in Chart 3.

niosomes system by themselves, being similar with that of DCP. Totally, the niosomal system in this study showed a good stability without DCP.

3.6. Release of SA and p-BA in vitro

Usually, the drug release rate can be affected by a few factors such as the buffering media, the characters of the membrane material, particle size and internal structure of the niosomes (Shi et al., 2006).

The release of encapsulated SA and *p*-BA from Span 60 niosomes has been observed. In simulated intestinal fluid (SIF), about 100% of free SA in solution form was released in 2 h whereas about 30% of SA was released from niosomes within 24 h (Fig. 4a). Obviously, the release rates of SA from the niosome formulations, in simulate intestinal fluid, were significantly slower compared to free drug solution ($P < 0.05$). Similarly, in simulated gastric fluid (SGF), the release studies also indicated that almost 100% of SA was released in 1 h in free solution, while about 20% of SA was released from the niosomal system by the end of the experiment (Fig. 4b). Comparing the SA release from niosome in these two kinds of simulated fluid, the drug release rate in SGF is apparently slower than that in SIF ($P < 0.05$). It could be attributed to the different structural forms of SA at different pH values. Considering that pK_{a1} value of SA is 2.97, it is obvious that almost all the SA molecules remain neutral state in SGF since the SGF pH is 1.2 (Fig. 5a). And SA molecules could be entrapped in the internal aqueous core or intercalated within the bi-layer structure of niosomal membrane. Under the condition of SIF (pH 7.5), the carboxyl group of SA was fully ionized (Chart 3a, structure II) and it was only entrapped in the internal aqueous core of niosome. Thus, the lower release rate in gastric fluid media than that in SIF indicated the preference of entrapment of unionized salicylic acid in niosome particles (Junyaprasert et al., 2008; Mokhtar et al., 2008).

Interestingly, the release trend of *p*-BA was opposite to that of SA. The release rate of *p*-BA from niosomes in SIF (Fig. 4c) was apparently slower than that in SGF (Fig. 4d) ($P < 0.05$), and the release profile of *p*-BA in SGF was almost the same as that of SA (Fig. 4b). As an isomer of SA, the neutral *p*-BA molecules (Chart 3b, structure IV) were also encapsulated in internal aqueous core or intercalated into the membrane of niosome in SGF. The related mechanism would be discussed in the next section.

These release experimental results clearly shown that the release of both SA and *p*-BA were greatly retarded in niosome system. Therefore, the side effects of drugs could be reduced and these niosome systems could be applied as effective drug carriers.

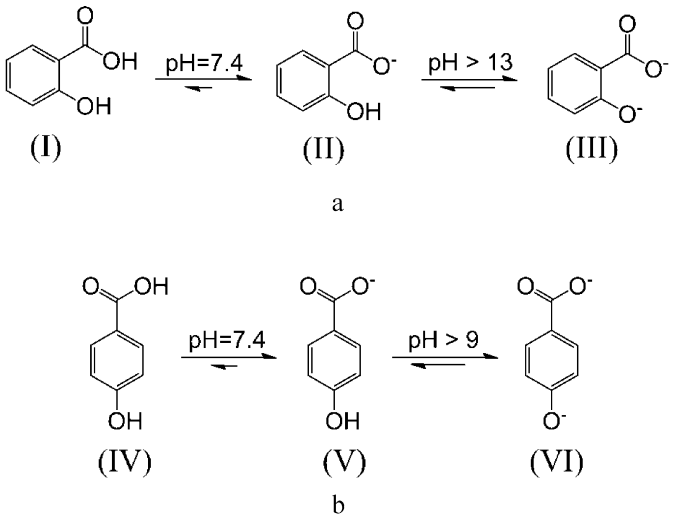

Chart 3. The structural transformation equilibrium of salicylic acid (a) and *p*-hydroxyl benzoic acid (b) at different pH values.

3.7. Possible mechanism of encapsulation and release of SA and p-BA from niosome

To obtain further insights into different capability of niosome in encapsulation SA and *p*-BA, the species distribution have been calculated at different pH values based on the pK_a values of SA and *p*-BA and the corresponding distribution curves were shown in Fig. 5. According to Fig. 5a, in PBS buffer solution (pH 7.4), carboxyl group of SA lost its proton, then a mono-charged species (II) obtained (Chart 3a), and the content of mono-charged species of SA (II) was almost 100%. Then, the intramolecular hydrogen bond formed between carboxyl and adjacent hydroxyl group in SA (Chart 4a). This kind of intramolecular hydrogen bond is very stable, preventing SA molecule from further interaction with other SA molecule or membrane molecules.

Being similar with SA, according to Fig. 5b, in PBS buffer solution with pH 7.4, carboxyl group of *p*-BA also lost its proton, then a mono-charged species (V) obtained (Chart 3b), and the content of mono-charged species of *p*-BA (V) was about 98.8%. As a result, the intermolecular hydrogen bonds formed between carboxyl and hydroxyl group in different *p*-BA molecules (Chart 4b), which this type of intermolecular hydrogen bonding has been found in many previous reports (Fukuyama et al., 1973; Parshad et al., 2004; Quah et al., 2008). The carboxyl terminus of the long chain structure (Chart 4b) could interact with hydroxyl of Span molecules *via* hydrogen bonding interactions (Loftsson et al., 1996), and this interaction was illustrated in Scheme 1. Comparing with those of SA, the higher EE% and slower release rate of *p*-BA maybe attributed to the intermolecular interactions between niosome membrane and solutes.

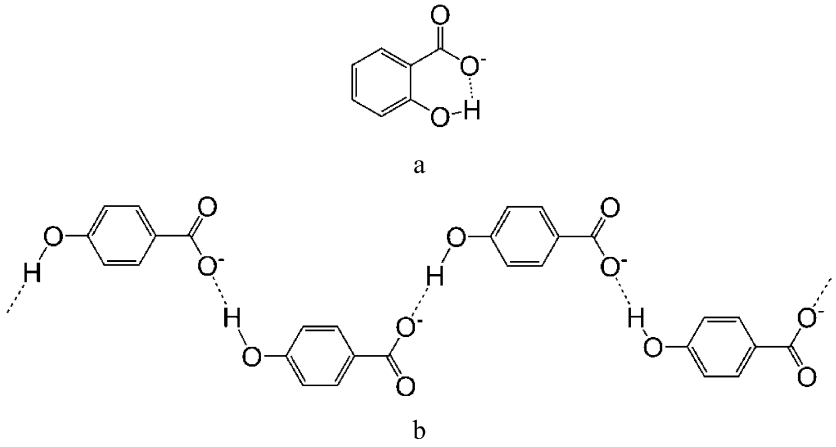

Chart 4. Hydrogen bonding interactions of salicylic acid (a) and *p*-hydroxyl benzoic acid (b) in PBS buffer solution of pH 7.4.

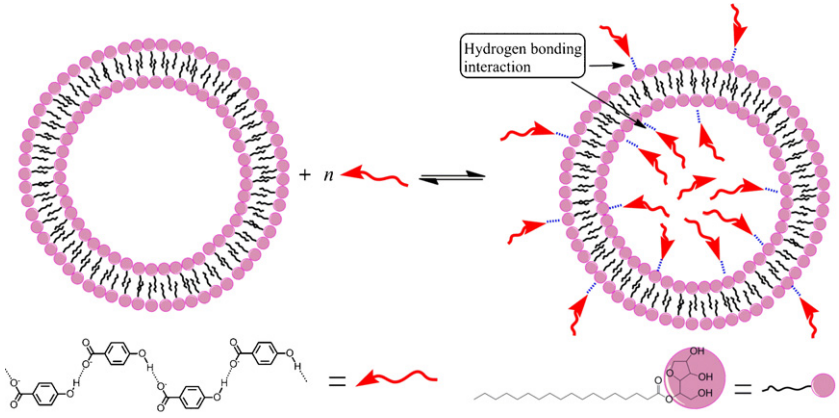

Scheme 1. Proposed hydrogen bonding interactions between membrane of niosome and *p*-BA molecules.

3.8. UV spectroscopy study of interaction between niosome membrane and solutes

To verify the interactions between membrane of niosome and solutes, UV spectroscopy measurements have been performed, and the corresponding UV absorption spectra are given in Fig. 6.

From the Fig. 6, the absorption peak of free *p*-BA is 247 nm, and the peak of *p*-BA entrapped in niosome is 240 nm, which has a 7 nm shift towards the short wavelength region. This variation should be attributed to the strong interaction between niosome membrane and *p*-BA molecules. According to the structure of *p*-BA and components of niosome (Span 60 and CH), only the hydrogen bonding could exist between niosome membrane and *p*-BA molecules. In previous reports (Stalin et al., 2005), it was also observed that hydrogen bonding interaction led to blue shift of UV absorption spectrum. For SA system, the absorption peaks of SA-niosome and free SA solution have same position (295 nm). The results of UV absorption spectroscopy proved indirectly that there are intermolecular interactions between niosome membrane and *p*-BA, but no apparent interaction was observed between niosome and SA.

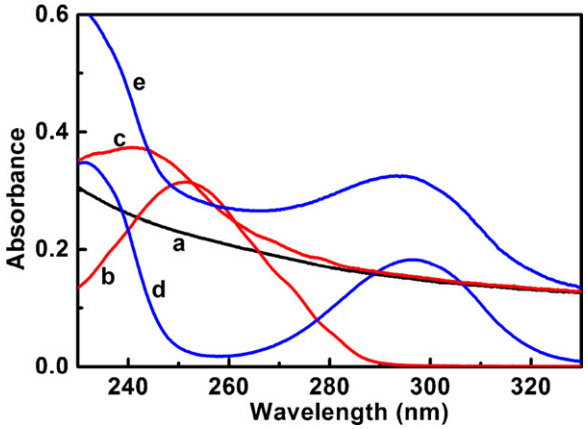

Fig. 6. UV absorption spectra of (a) blank niosome, (b) *p*-BA, (c) *p*-BA-niosome, (d) SA, and (e) SA-niosome.

3.9. Quantitative analysis of hydrogen bonding interaction between niosome membrane and solutes to entrapment extent

In a whole niosome system containing solutes, solutes can be divided into three parts at equilibrium:

(1) Untrapped solute, which locates outside of niosome and can be removed by dialysis.
(2) Entrapped solute, which locates inside of niosome and cannot be removed by dialysis. There are no interaction between niosome and solute.
(3) Solute molecules interacting with niosome, and cannot be removed by dialysis.

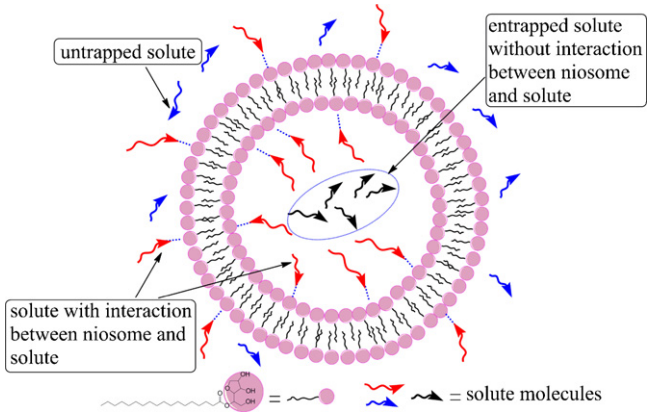

Fig. 7. The relationship diagram among untrapped solute, entrapped solute without interaction with niosome membrane, solute having interaction with niosome membrane.

The relationship diagram is shown in Fig. 7.

For niosome made from Span 60 and CH, the entrapment equilibrium can be described clearly by the following equation:

$$\text{Span} + \text{solute} \overset{K}{\rightleftharpoons} \text{solute-Span} + \text{solute@Span} \quad (2)$$

where solute-Span denotes the species of solute molecules interacting with niosome; solute@Span represents the species of entrapped solute without interaction with niosome membrane, and K is the equilibrium constant.

For equilibrium equation (2), the initial concentrations of Span (Here, Span presents total lipid), solute, solute-Span and solute@Span can be described in $[\text{Span}]_0$, $[\text{solute}]_0$, 0, and 0 mol dm^{-3}, respectively. Similarly, the equilibrium concentrations of Span, solute, solute-Span and solute@Span can be described in $[\text{Span}]_e$, $[\text{solute}]_e$, $[\text{solute-Span}]_e$, and $[\text{solute@Span}]_e$ mol dm^{-3}, respectively.

According to the material balance, at an equilibrium state,

$$[\text{Span}]_e = [\text{Span}]_0 - [\text{solute-Span}]_e \quad (3)$$

$$[\text{solute}]_0 = [\text{solute}]_e + [\text{solute-Span}]_e + [\text{solute@Span}]_e \quad (4)$$

$$K = \frac{[\text{solute-Span}]_e[\text{solute@Span}]_e}{[\text{Span}]_e[\text{solute}]_e} = \frac{[\text{solute-Span}]_e([\text{solute}]_0 - [\text{solute}]_e - [\text{solute-Span}]_e)}{([\text{Span}]_0 - [\text{solute-Span}]_e)[\text{solute}]_e} \quad (5)$$

Eq. (5) can be transformed into the following equation:

$$[\text{solute}]_0 = \frac{K[\text{Span}]_0}{[\text{solute-Span}]_e}[\text{solute}]_e + [\text{solute-Span}]_e \quad (6)$$

When the solute is p-BA or SA, the corresponding $[\text{solute}]_e$ can be measured by UV absorption spectroscopy. Under the same initial concentration of Span, a series of values of $[\text{solute}]_e$, can be obtained by changing the different initial concentration $[\text{solute}]_0$ of p-BA or SA. By plotting $[\text{solute}]_0$ *vs.* $[\text{solute}]_e$, the thermodynamic equilibrium constant K and $[\text{solute-Span}]_e$ can be calculated from the slope and intercept (Fig. 8). For p-BA and SA in Span niosome system at room temperature, the corresponding equilibrium constants K are 1.54 and 0.17, respectively. The concentrations of p-BA and SA interacting with Span niosome by hydrogen bonding are 1.208×10^{-4}, and 0.414×10^{-4} mol dm^{-3} ($[\text{Span}]_0 = 2.0 \times 10^{-4}$ mol dm^{-3}). It means that the ratio of p-BA which binds with niosome by hydrogen bonding to total lipid reaches 60.4%, and this value of SA is 20.7%. The entrapment and release of both solutes were influenced greatly by the hydrogen binding interaction intensity. The stronger hydrogen binding, the higher entrapment efficiency is.

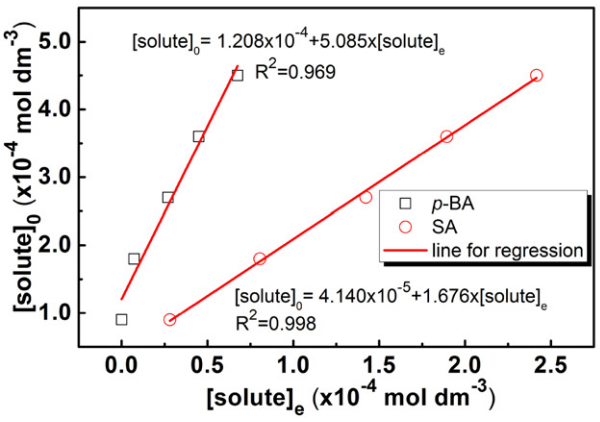

Fig. 8. Plot of $[\text{solute}]_0$ *vs.* $[\text{solute}]_e$ to calculate equilibrium constant K and $[\text{solute-Span}]_e$ for entrapment equilibria of p-BA, SA model solutes in niosome. ($[\text{Span}]_0 = 2.0 \times 10^{-4}$ mol dm^{-3}; temperature, 25 ± 2 °C; the initial concentration range of p-BA or SA was $0.9–4.5 \times 10^{-4}$ mol dm^{-3}.).

4. Conclusions

Being different from previous researches, the current study mainly indicates the importance of hydrogen bonding interactions of solutes in the encapsulation and release. Here SA and its isomer p-BA were used as models and the corresponding encapsulation efficiency were evaluated and compared. The quantitative analysis of hydrogen binding interaction between solute and niosome has been finished firstly, and the corresponding entrapment equilibrium constant has been calculated. The results demonstrated that the hydrogen bonding interaction between drugs and membrane molecules is greatly helpful to improve the encapsulation efficiency of drugs and reduce the release rate. This study provides a new insight into designing effective niosomal system.

Acknowledgments

This work was supported by the National Basic Research Program of China (973 Program) 2006CB705601, foundation of Graduate University of Chinese Academy of Sciences (110300N000) and by a grant from the State Key Laboratory of Environmental Chemistry and Ecotoxicology, Research Center for Eco-Environmental Sciences, Chinese Academy of Sciences (KF2008-04).

References

Abd-Elbary, A., El-laithy, H.M., Tadros, M.I., 2008. Sucrose stearate-based proniosome-derived niosomes for the nebulisable delivery of cromolyn sodium. Int. J. Pharm. 357, 189–198.

Aggarwal, D., Garg, A., Kaur, I.P., 2004. Development of a topical niosomal preparation of acetazolamide: preparation and evaluation. J. Pharm. Pharmacol. 56, 1509–1517.

Alsarra, I.A., 2009. Evaluation of proniosomes as an alternative strategy to optimize piroxicam transdermal delivery. J. Microencapsul. 26, 272–278.

Arunothayanun, P., Bernard, M.S., Craig, D.Q.M., Uchegbu, I.F., Florence, A.T., 2000. The effect of processing variables on the physical characteristics of non-ionic surfactant vesicles (niosomes) formed from a hexadecyl diglycerol ether. Int. J. Pharm. 201, 7–14.

Arunothayanun, P., Turton, J.A., Uchegbu, I.F., Florence, A.T., 1999. Preparation and in vitro in vivo evaluation of luteinizing hormone releasing hormone (LHRH)-loaded polyhedral and spherical tubular niosomes. J. Pharm. Sci. 88, 34–38.

Assadullahi, T.P., Hider, R.C., Mcauley, A.J., 1991. Liposome formation from systhetic polyhydroxyl lipids. Biochim. Biophys. Acta 1083, 271–276.

Azmin, M.N., Florence, A.T., Handjani-Vila, R.M., Stuart, J.F.B., Vanlerberghe, G., Whittaker, J.S., 1985. The effect of non-ionic surfactant vesicle (niosome) entrapment on the absorption and distribution of methotrexate in mice. J. Pharm. Pharmacol. 37, 237–242.

Bandak, S., Ramu, A., Barenholz, Y., Gabizon, A., 1999. Reduced UV-induced degradation of doxorubicin encapsulated in polyethyleneglycol-coated liposomes. Pharm. Res. 16, 841–846.
Bandyopadhyay, P., Johnson, M., 2007. Fatty alcohols or fatty acids as niosomal hybrid carrier: effect on vesicle size, encapsulation efficiency and in vitro dye release. Colloid Surf. B: Biointerfaces 58, 68–71.
Barakat, H.S., Darwish, I.A., El-Khordagui, L.K., Khalafallah, N.M., 2009. Development of naftifine hydrochloride alcohol-free niosome gel. Drug Dev. Ind. Pharm. 35, 631–637.
Bayindir, Z.S., Yuksel, N., 2010. Characterization of niosomes prepared with various nonionic surfactants for paclitaxel oral delivery. J. Pharm. Sci. 99, 2049–2060.
Degier, J., Mandersloot, J.G., Vandeene, L.L., 1968. Lipid composition and permeability of liposomes. Biochim. Biophys. Acta 150, 666–668.
EL-Samaligy, M.S., Afifi, N.N., Mahmoud, E.A., 2006. Increasing bioavailability of silymarin using a buccal liposomal delivery system: preparation and experimental design investigation. Int. J. Pharm. 308, 140–148.
Fenton, R.R., Easdale, W.J., Meng, H., Omara, E.S.M., Mckeage, M.J., Russell, P.J., Hambley, T.W., 1997. Preparation, DNA binding, and in vitro cytotoxicity of a pair of enantiomeric platinum(II) complexes. [(R)- and (S)-3-aminohexahydroazepine]dichloro- platinum(II). Crystal structure of the S enantiomer. J. Med. Chem. 40, 1090–1098.
Fukuyama, K., Kashino, S., Haisa, M., 1973. Crystal-structure of piperdinium parahydroxybenzoate. Acta Crystallogr. Sect. B 29, 2713–2717.
Gude, R.P., Jadhav, M.G., Rao, S.G.A., Jagtap, A.G., 2002. Effects of niosomal cisplatin and combination of the same with theophylline and with activated macrophages in murine B16F10 melanoma model. Cancer Biother. Radiopharm. 17, 183–192.
Hao, Y.M., Zhao, F.L., Li, N., Yang, Y.H., Li, K.A., 2002. Studies on a high encapsulation of colchicine by a niosome system. Int. J. Pharm. 244, 73–80.
Hong, M.H., Zhu, S.J., Jiang, Y.Y., Tang, G.T., Pei, Y.Y., 2009. Efficient tumor targeting of hydroxycamptothecin loaded PEGylated niosomes modified with transferring. J. Control. Release 133, 96–102.
Hu, C.J., Rhodes, D.G., 1999. Proniosomes: a novel drug carrier preparation. Int. J. Pharm. 185, 23–35.
Junyaprasert, V.B., Teeranachaideekul, V., Supaperm, T., 2008. Effect of charged and non-ionic membrane additives on physicochemical properties and stability of niosomes. AAPS PharmSciTech 9, 851–859.
Loftsson, T., Fridriksdottir, H., Gudmundsdottir, K., 1996. The effect of water-soluble polymers on aqueous solubility of drugs. Int. J. Pharm. 127, 293–296.
Mainardes, R.M., Silva, L.P., 2004. Drug delivery systems: past, present, and future. Curr. Drug Targets 5, 449–455.
Manconi, M., Sinico, C., Valenti, D., Lai, F., Fadda, A.M., 2006. Niosomes as carriers for tretinoin III. A study into the in vitro cutaneous delivery of vesicle-incorporated tretinoin. Int. J. Pharm. 311, 11–19.
Manosroi, A., Chutoprapat, R., Abe, M., Manosroi, J., 2008. Characteristics of niosomes prepared by supercritical carbon dioxide ($scCO_2$) fluid. Int. J. Pharm. 352, 248–255.
Manosroi, A., Wongtrakul, P., Manosroi, J., Midorikawa, U., Hanyu, Y., Yuasa, M., Sugawara, F., Sakai, H., Abed, M., 2005. The entrapment of kojic oleate in bilayer vesicles. Int. J. Pharm. 298, 13–25.
Mokhtar, M., Sammour, O.A., Hammad, M.A., Megrab, N.A., 2008. Effect of some formulation parameters on flurbiprofen encapsulation and release rates of niosomes prepared from proniosomes. Int. J. Pharm. 361, 104–111.
Nasr, M., Mansour, S., Mortada, N.D., Elshamy, A.A., 2008. Vesicular aceclofenac systems: a comparative study between liposomes and niosomes. J. Microencapsul. 25, 499–512.
Paolino, D., Cosco, D., Muzzalupo, R., Trapasso, E., Picci, N., Fresta, M., 2008. Innovative bola-surfactant niosomes as topical delivery systems of 5-fluorouracil for the treatment of skin cancer. Int. J. Pharm. 353, 233–242.
Paolino, D., Muzzalupo, R., Ricciardi, A., Celia, C., Picci, N., Fresta, M., 2007. In vitro and in vivo evaluation of bola-surfactant containing niosomes for transdermal delivery. Biomed. Microdev. 9, 421–433.
Pardakhty, A., Varshosaz, J., Rouholamini, A., 2007. In vitro study of polyoxyethylene alkyl ether niosomes for delivery of insulin. Int. J. Pharm. 328, 130–141.
Parshad, H., Frydenvang, K., Liljefors, T., Sorensen, H.O., Larsen, C., 2004. Aqueous solubility study of salts of benzylamine derivatives and *p*-substituted benzoic acid derivatives using X-ray crystallographic analysis. Int. J. Pharm. 269, 157–168.
Quah, C.K., Jebas, S.R., Fun, H.K., 2008. 3-Aminobenzoic acid-4-nitrobenzoic acid (1/1). Acta Crystallogr. Sect. E 64, o2230–U2292.
Shi, B., Fang, C., Pei, Y.Y., 2006. Stealth PEG-PHDCA niosomes: effects of chain length of PEG and particle size on niosomes surface properties, in vitro drug release, phagocytic uptake, in vivo pharmacokinetics and antitumor activity. J. Pharm. Sci. 95, 1873–1887.
Speight, J.G., 2005. Lange's Handbook of Chemistry, 16th ed. McGraw-Hill, New York.
Stalin, T., Devi, R.A., Rajendiran, N., 2005. Spectral characteristics of ortho, meta and para dihydroxy benzenes in different solvents, pH and beta-cyclodextrin. Spectrochim. Acta Part A: Mol. Biomol. Spectrosc. 61, 2495–2504.
Uchegbu, I.F., Vyas, S.P., 1998. Non-ionic surfactant based vesicles (niosomes) in drug delivery. Int. J. Pharm. 172, 33–70.
Vora, B., Khopade, A.J., Jain, N.K., 1998. Proniosome based transdermal delivery of levonorgestrel for effective contraception. J. Control. Release 54, 149–165.
Zhao, Y., Zheng, Y.J., Gao, B., Yi, D., 1998. The inhibition effect of *p*-hydroxybenzoic acid on tyrosinase. Acta Sci. Nat. Univ. Jilin 4, 89–90.